

Experiment and Numerical Simulation of Gas-Liquid Flow in Microchannels

Multiphase flows in microfluidic devices have received much attention because of the foreseeable advantages that unique microscale properties have to offer with regard to enhanced heat and mass transfer efficiency, reduced axial dispersion, and smaller sample volume. In order to realize these benefits, a good understanding of the complex multiphase flow behavior in microfluidic devices must be developed. In our recent study, the behavior of gas-liquid flow in a microchannel is investigated using both microscopic imaging and Lattice Boltzmann simulation techniques.

The experiment setup for the microfluidic experiment is shown schematically in Figure 1(a). The microchannels were fabricated in polymethyl methacrylate (PMMA) using an Aerotech ultra precision micromilling system with 125 and 250 micron bits for the channels and a 1 millimeter bit for the inlet and outlet. All channels were 125 microns deep and were sealed by thermo bonding a transparent thin film of PMMA. Inlet and outlet ports were glued over the inlet and outlet holes with 1/8" barbed tubing ports. The liquid inlet was immediately split into 2 channels that traveled around the air inlet and converged at the mixing zone, which had a cross shape. A dual syringe pump was used to push the liquid and air streams into the microchannels. When setting a new flow rate, the system was allowed to run for 5 minutes to reach a steady state before images were taken. Images were captured using an inverted microscope with a 4x objective and a high speed CMOS camera capable of 1000 frames per second at full resolution.

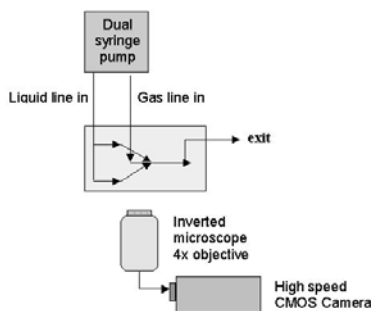


Figure 1. Schematic illustration of the experiment setup.

Figure 2 shows three typical images of bubbles obtained in the experiments at different Capillary number (Ca) and flow rate ratios. It is observed that small, dispersed bubbles are usually formed at higher Ca , while gas slugs are often associated with lower Ca . This phenomenon is

consistent with previous studies in the literature. The detailed characteristics and bubble formation mechanisms in these two regimes are described in the following sections.

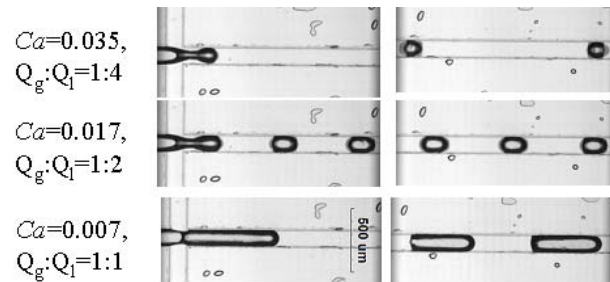


Figure 2. Air-sugar solution system in microchannels. The width of the channels is 125 μ m. For each case, the picture on the left shows the mixing section, and the picture on the right shows the downstream of the channel where the bubble reached a stable shape

The bubble formation process for $Ca=0.04$ is shown in Figure 3(a). The experiment was conducted in a cross-shaped channel 250 μ m in width using sugar solution as the liquid phase. The formation of the bubble started with the co-flow of the gas and liquid in the mixing section. After the front of the gas stream entered the main channel, the tip of the gas phase kept expanding, and the neck connecting the bubble tip and the gas stream kept thinning. The thinning of the neck ultimately led to the breakup of the bubble from the gas stream. In this case, the breakup point is located in the main channel after the mixing section, and the width of the bubble is almost the same as the width of the channel. The bubble formation process was also simulated under the similar Ca number and flowrate ratio, as shown in Figure 3(b). The simulation was able to reproduce the shape of the bubble during the formation as well as the location of the breakup point.

When Ca was decreased, the surface tension force started to dominate over the viscous force. As a result, the gas-liquid interface was able to expand to the undeformed shape after the mixing section, almost blocking the entire liquid flow. This, in turn, led to increased pressure in the liquid phase, and this increased pressure enabled the liquid to pinch off the gas stream and form gas slugs. This mechanism for bubble formation by pressure drop was believed to be the main mechanism for bubble formation at low Ca numbers. Figure 4(a) shows the simulated snapshots of the bubble formation under the condition $Ca=0.006$, and $Q_g:Q_l=1:2$. It was observed that after mixing the gas phase is in the slug shape, which had a much larger contact area with the channel wall compared

to the bullet shape bubbles. The breakup point was located at the end of the mixing section, rather than in the downstream channel as in the previous case in Figure 3.

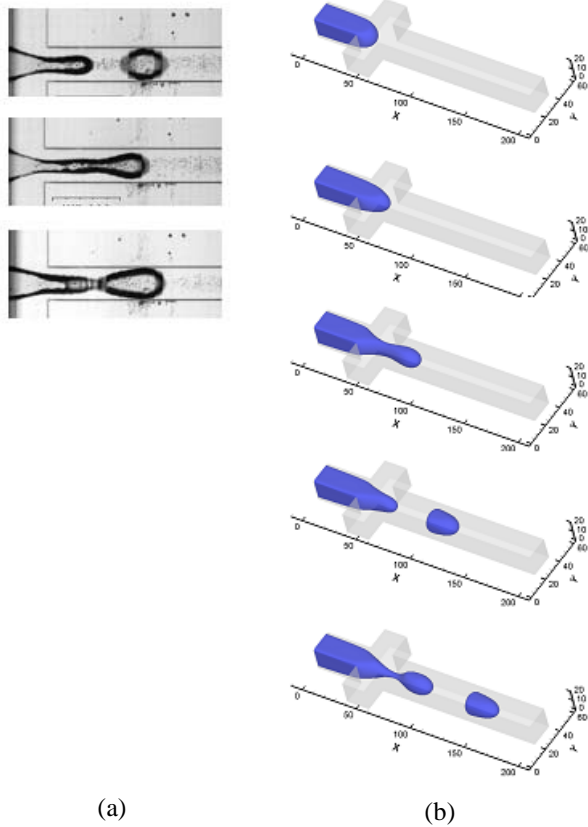


Figure 3. (a) Air bubble formation in sugar solution in 250 μ m channel. $Ca=0.04$. $Q_g:Q_l=1:2$. (b) 3D LBM simulation results for $Ca=0.03$, $Q_g:Q_l=1:2$.

In order to verify the pressure-drop-induced bubble formation mechanism, the pressure profiles at the gas inlet and the liquid inlet were extracted from the simulation data. The variation of the pressure at the gas and liquid inlet with time is shown in Figure 4(b), in which the corresponding time points to the snapshots in Figure 4(a) are also marked.

It is clear that during the waiting period (before the gas stream went past the mixing section), the pressure in the gas inlet was always higher than that in the liquid, because of the Laplace pressure across the concave interface (point A). As the interface advanced, the pressure difference in the two phases decreased because of the decrease of the interface curvature. Once the gas stream passed the mixing region and blocked the liquid flow, the pressure in liquid started to rise. The interface also changed from concave to convex, and therefore the liquid pressure became higher than the gas pressure (point B). The liquid pressure reached its maximum near the time when the width of the gas stream was minimum

(point C). When the bubble broke away from the gas stream, the liquid pressure dropped while the gas pressure went up. The gas inlet pressure again became higher than the liquid inlet pressure (point D). The previous bubble formation cycle was also included in the same figure, which showed a consistent pattern of pressure fluctuation. The pressure difference in the two phases could be interpreted using the Laplace pressure, indicating that the bubble formation process could be viewed as a series of equilibrium states. The variation of pressure with time confirmed the hypothesis that the pressure difference was the main mechanism for bubble formation at the low Ca number.

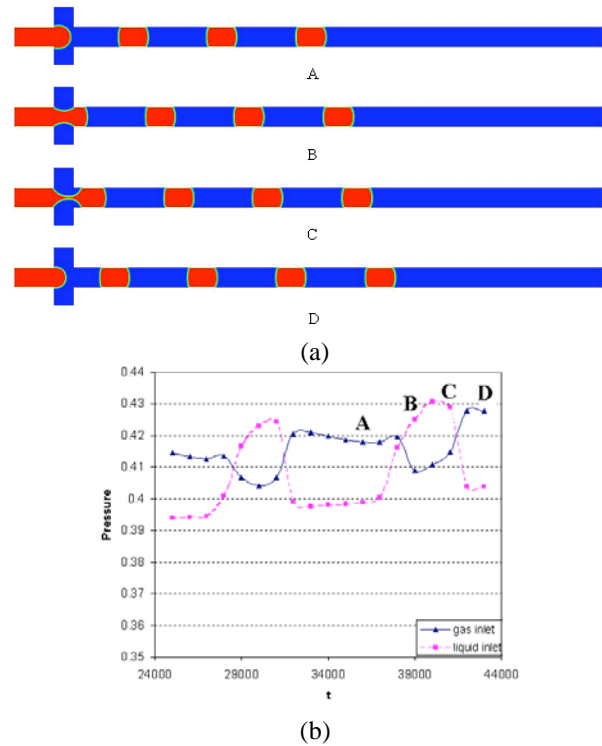


Figure 4. Simulation results for $Ca=0.006$, $Q_g:Q_l=1:2$. (a) Snapshots of the bubble formation process. (b) Pressure variation at the gas and liquid inlet during bubble formation, time points A to D correspond to the four snapshots in (a)

Publications

1. Yu, Z, Hemminger, O, Fan, LS, 2007, Experiment and lattice Boltzmann simulation of two-phase gas-liquid flows in microchannels, *Chemical Engineering Science*, 6(24), 7172-7183